

1      **Separation of an upwelling current bounding the Juan  
2      de Fuca Eddy**

3      **Jody M. Klymak<sup>1,2</sup>, Susan E. Allen<sup>3,4</sup>, Stephanie Waterman<sup>3</sup>**

4      <sup>1</sup>School of Earth and Ocean Sciences, University of Victoria, BC, Canada

5      <sup>2</sup>Department of Physics & Astronomy, University of Victoria, BC, Canada

6      <sup>3</sup>Department of Earth, Ocean and Atmospheric Sciences, University of British Columbia, Vancouver, BC,

7      Canada

8      <sup>4</sup>Institute of Applied Mathematics, University of British Columbia, Vancouver, BC, Canada

9      **Key Points:**

- 10     • The shelf break current along Vancouver Island separates downstream of a submarine  
11     bank.
- 12     • Offshore water is drawn onto the shelf and forms a sharp semi-persistent front with  
13     the Juan de Fuca Eddy.
- 14     • The Eddy shows evidence of long residence times, and little evidence of deep-water  
15     origin.

16 **Abstract**

17 Observations of temperature, salinity, and oxygen on the southern Vancouver Island  
 18 shelf show a large-scale exchange of shelf water with offshore water, just offshore of a semi-  
 19 permanent recirculation. The semi-permanent cyclonic recirculation (the Juan de Fuca  
 20 Eddy) occupies a region where the shelf widens abruptly in the lee of a bank. The water  
 21 in this Eddy is a mixture of offshore water and water from a buoyant coastal current. This  
 22 water is well-mixed along a mixing line in temperature-salinity space, though it retains  
 23 stratification, and is either rapidly mixed or has a long residence time. There is a sharp  
 24 temperature-salinity front on the offshore side of this well-mixed water, no more than 1-km  
 25 wide, and has no sign of instabilities. The clearest evidence of cross-front transport is found  
 26 during a short tidally resolved survey over a bank, and was due to flows in the cross-bank  
 27 direction driving large mixing in 50-m tall hydraulic jumps. Upstream of the recirculation  
 28 there is an along-shelf current flowing equatorward. However the whole current separates  
 29 from the shelf before reaching the recirculation, in the lee of a bank, and is replaced by  
 30 water from offshore. The separation event was also seen in sea-surface temperatures from  
 31 satellite images as a tongue of cool coastal water that is ejected offshore.

32 **Plain Language Summary**

33 The southern Vancouver Island continental shelf is biologically productive due to high  
 34 nutrient input from the Strait of Juan de Fuca and Salish Sea estuarine system and sub-  
 35 stantial cross-shelf transport due to the complicated topography. Here we present intensive  
 36 sampling of the Juan de Fuca Eddy region. The observations show that below the surface  
 37 mixed layer, the water in the Eddy is low in oxygen, and has undergone substantial vertical  
 38 and lateral mixing. In contrast to previous literature we find that the low oxygen in the  
 39 eddy is likely because of respiration rather than being pulled from low-oxygen water in the  
 40 California Undercurrent.

41 The observations also show a remarkable flow separation of the equatorward shelf  
 42 current. The current is seen to detach and is pushed offshore. Such events are readily seen  
 43 in satellite imagery, but our observations indicate that the separation extends the depth of  
 44 the water column on the shelf, and that this separation may be partially driven by the local  
 45 bathymetry. The separation is a very strong cross-shelf exchange event, and transports  
 46 substantial nutrient-rich coastal water offshore to drive productivity in the deeper ocean  
 47 adjacent to the continental slope.

48 **1 Introduction**

49 Cross-shelf exchange is important to the health and productivity of continental shelf  
 50 regions, allowing for offshore oxygenated water to be exchanged with nutrient-rich, but  
 51 oxygen-depleted, nearshore water. Cross-shelf transport usually requires ageostrophic flow,  
 52 since geostrophically balanced flow will tend to follow topographic contours, often providing  
 53 a barrier to lateral exchange (Brink, 2016). Mechanisms of cross-shelf exchange include  
 54 internal waves and instabilities in shelf-break fronts. However, these mechanisms can be  
 55 smaller in magnitude compared to intermittent three-dimensional exchange, driven by ed-  
 56 dying, often catalyzed by topographic irregularity (Barth et al., 2000).

57 Here we present detailed *in-situ* observations from the southern Vancouver Island shelf,  
 58 collected in summer 2013, and sampled by a rapid profiling vehicle equipped with a CTD  
 59 and oxygen sensor, supplemented by traditional hydrographic surveys bracketing the high  
 60 resolution observations by a month. The shelf has complicated bathymetry (figure 1), with  
 61 a relatively simple 50-km wide shelf poleward of our study site, that widens to over 75 km  
 62 wide equatorward of La Perouse Bank. The South Vancouver Island Shelf is this wide shelf  
 63 region, characterized by a number of banks, and finally is incised on the poleward side by the

64 Juan de Fuca canyon. Water from the Strait of Juan de Fuca flows poleward as a buoyant  
 65 current that hugs the coast (Thomson et al., 1989; Hickey et al., 1991), while shelf water  
 66 flows equatorward in the summer both forced by local winds and via teleconnections with  
 67 the long, homogenous shelves equatorward off Washington and Oregon (Hickey et al., 1991;  
 68 Thomson & Krassovski, 2015; Engida et al., 2016). Trapped between these two currents  
 69 is a region of relatively homogenous water that has been termed the Juan de Fuca Eddy  
 70 (Freeland & Denman, 1982; Freeland & McIntosh, 1989; Foreman et al., 2008; MacFadyen  
 71 & Hickey, 2010), denoted “EDDY” below.

72 A goal of our study was to understand how the EDDY persists and how it exchanges  
 73 water properties with offshore water. We focus on water deeper than 50m, below the summer  
 74 mixed layer, because this water is trackable with water mass properties, even though the  
 75 EDDY is often studied from the point of view of the surface circulation (MacFadyen & Hickey,  
 76 2010). Past studies have found low oxygen concentrations in the EDDY, and inferred that  
 77 water is upwelled from the California Undercurrent from as deep as 400 m (Freeland &  
 78 Denman, 1982; Dewey & Crawford, 1988). This inference was based on the assumption  
 79 that oxygen is conservative, and hence water in the EDDY had to come from the oxygen  
 80 minimum zone found further offshore (Mackas et al., 1987). This lead to hypotheses that  
 81 perhaps the EDDY was fed by waters being drawn up a spur canyon (called the Spur Canyon)  
 82 via ageostrophic transport from offshore to onshore due to low pressure in the EDDY center  
 83 (Weaver & Hsieh, 1987). Below, we will argue that there is no evidence of such transport  
 84 and that oxygen is likely low because of local consumption due to respiration.

85 A second goal of our study was to better understand cross-shore exchange between  
 86 shelf and offshore water. Cross-shore transport is supplied by Ekman layers in simple ge-  
 87ometries under wind forcing. However, in many locations there is also evidence of eddies  
 88 and filaments driving wholesale separation of shelf currents into the deep ocean. Along  
 89 the Vancouver Island shelf, large filaments or instabilities of the coastal current have been  
 90 inferred using satellite images (Ikeda & Emery, 1984; Thomson & Gower, 1998). Direct  
 91 observations of such filaments have been made further to the south off Cape Blanco (Barth  
 92 et al., 2000), and off other coasts (Relvas & Barton, 2005). Net cross-shore transport of  
 93 nutrients and chlorophyll have been found in hydrographic surveys off Vancouver Island  
 94 (Mackas & Yelland, 1999), and associated with mesoscale features in geostrophic velocities  
 95 and in satellite observations. The mechanisms driving such separations are poorly un-  
 96 derstood, but hypotheses include coastal hydraulics leading to along-shore trapping of coastal  
 97 waves (Dale & Barth, 2001), wind stress curl variations (Castelao & Barth, 2007), induced  
 98 relative vorticity due to stretching of parcels that overshoot their initial isobaths due to  
 99 a sudden change in downstream bathymetry (D’Asaro, 1988), and, at this location, non-  
 100 linear breaking of large-scale meanders due to baroclinic instability between the wind-driven  
 101 current and the California Undercurrent (Ikeda et al., 1984; Battean, 1997).

102 In this paper we present observations of water masses on the Southern Vancouver Island  
 103 Shelf collected in 2013 (section 2), presenting the data in a number of ways to highlight the  
 104 important processes, with a focus on the offshore side of the EDDY region (section 3) where  
 105 we consider the age of the EDDY, the steadiness of the front separating the EDDY and the  
 106 offshore water, properties along the spur canyon that was believed to feed the EDDY, and  
 107 a large offshore tongue of the shelf-break current and its intrusion into the interior. We  
 108 discuss the origin of the EDDY and the implications of the separating jet (section 4).

## 109 2 Site and Methods

110 The study site was the southern portion of the Vancouver Island Shelf (figure 1a), a  
 111 particularly complicated region due to the bathymetry and varied forcing. At the south end  
 112 of the study site is the Juan de Fuca canyon, which feeds dense water into Juan de Fuca  
 113 Strait. This dense water is mixed with fresh water from the Fraser River at the sills and  
 114 archipelagos further inland and fluxes out the Strait again, where it turns poleward along

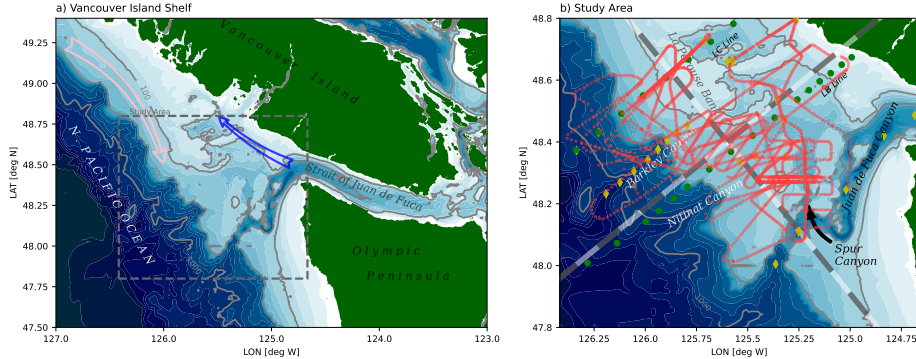


**Figure 1.** a) Study site on the Vancouver Island Shelf. The blue arrow indicates the direction of the Vancouver Island Coastal Current, and the pink arrow indicates southward flow of the coastal upwelling current. The dashed box indicates the approximate limits of the study area. b) The study area with hydrographic casts from the La Perouse cruises along the LB and LC Lines (green dots), hydrographic casts during the Falkor cruise (yellow diamonds), and finescale Moving Vessel Profiler casts (red dots). The coordinate system used for this paper is shown with alternating grey and white bands at 10-km intervals in the along- and cross-shore directions.

Vancouver Island to form the Vancouver Island Coastal Current. The Juan de Fuca Canyon has a notable spur canyon (Spur Canyon), that incises the shelf towards the north into the study site (figure 1b). The rest of the shelf is punctuated by a series of banks and shallow basins. La Perouse bank separates the outer shelf from a deeper inner basin and forms the poleward boundary off where the shelf widens abruptly south of 48.5 N. Equatorward, the shelf widens further, and the shelf break has a series of submarine canyons, in particular Nitnat Canyon and Barkley Canyon.

We present observations from La Perouse hydrographic surveys along the LB and LC lines, collected aboard the *CCGS Tully* from 2013-05-30 to 2013-05-31 (“May”), and 2013-09-07 to 2013-09-09 (“September”). These lines span the 50 m isobath to deep offshore, with casts every 7.5 km across shelf. The data comes from a lowered Seabird 9-11 CTD, with an SBE 43 oxygen sensor. Oxygen data have been corrected against bottle casts, and the CTD corrected for sensor offsets and thermal lags.

We focus on finescale surveys carried out between these hydrographic surveys, from 2013-08-21 to 2013-08-30. Data were collected from the *R/V Falkor* with an AML Oceanographic Moving Vessel Profiler (MVP). Data was collected analogously to data collected during similar field campaigns (Klymak et al., 2015, 2016; D’Asaro et al., 2018). The MVP was equipped with an AML Oceanographic CTD, and a Rinko Oxygen sensor with a 7-s response time foil. The MVP profiled to depths of 200 m or to within 5 m of the seafloor, whichever was shallower, and dropped at a speed of approximately  $3 \text{ m s}^{-1}$ . Data collection took place while the ship cruised at speeds between 5 and 8 kts, usually at around 6 kts, to enable fine horizontal spacing of the casts, with typical spacing of 800 m in deep water, and less in water shallower than 200 m. Data is reported for the downcast, which mostly follows a vertical path. The rapid speed of the profiling makes the oxygen measurements somewhat coarse, and probably biased due to the phase lag of the sensor, so we treat these qualitatively in this paper.

Unfortunately, neither vessel had an operational acoustic Doppler profiler during the cruises with which to make water velocity measurements.

143 Winds during the cruises were typical for the west coast of Vancouver Island, with  
 144 equatorward upwelling-favorable winds during July and early August (figure 2). During  
 145 the finescale survey, and for the week previous, the winds were intermittently downwelling  
 146 favorable. Note that this locale is strongly affected by coastally trapped waves from further  
 147 south, so doming of near-bottom isopycnals often persists despite local wind forcing, and  
 148 takes a finite amount of time to spin down (Thomson & Krassovski, 2015; Engida et al.,  
 149 2016).

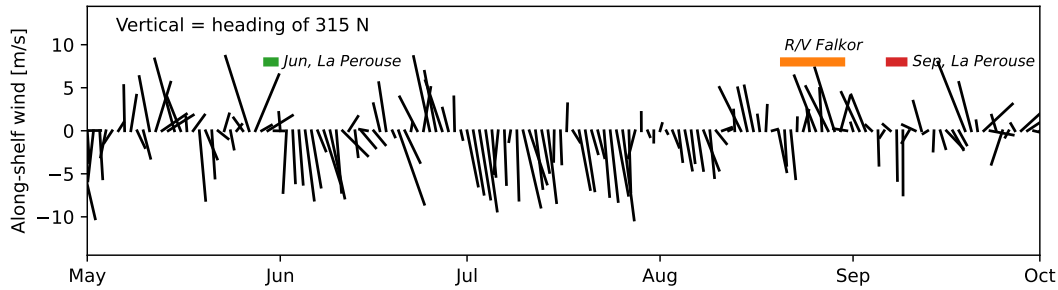


**Figure 2.** Wind from the La Perouse buoy (DFO, 2022). The vertical direction is along-shelf (chosen as a heading of 315 N), so vectors pointing straight down represent upwelling winds. The wind components have been low-pass filtered to one-day averages. The timing of the surveys discussed in the paper are shown as colored bands.

150

### 3 Observations

151

#### 3.1 Early and late summer hydrographic surveys

152 153 154 155 156 157 158

Hydrographic sections along the LB and LC hydrographic lines highlight summer conditions on the Southern Vancouver Island Shelf and indicate some of the features we are focusing on in this paper (Figure 3). During both surveys, and along both lines, there is clear evidence of upwelling, with the  $26.4 \text{ kg m}^{-3}$  isopycnal reaching from 130 m depth offshore to shallower than 85 m over the shelf. This upwelled water tends to be low in oxygen and cool. Further onshore, the Vancouver Island Coastal Current hugs the coast, where isopycnals tilt down towards the shore, and water is warmer than offshore.

159 160 161 162

The Juan de Fuca Eddy region is observed along the LB Line (figure 3, bottom three rows), mostly inshore of 0 km. This water is cooler and lower in oxygen than along the same isopycnal further offshore. Near the surface, the isopycnals are domed, and the low-oxygen anomaly extends as high as the thin surface mixed layer.

163 164 165 166 167 168 169 170

The water upstream of the EDDY region, along the LC line, is less mixed than the EDDY water (figure 3, top three rows). It does not show as much drawdown of oxygen, and is warmer, at least offshore of La Perouse bank ( $X \approx 5 \text{ km}$ ). Based on these properties, offshore water does not appear to make it over La Perouse bank into the onshore basin, or if it does, it does so intermittently and with substantial mixing. Note that the water along the  $26.4 \text{ kg m}^{-3}$  isopycnal becomes cooler and lower in oxygen where it intersects the shelf, consistent with both enhanced mixing near the shelf and with drawdown of oxygen by respiration.

171 172 173

The contrast in onshore and offshore waters can be clearly traced in temperature-salinity ( $\theta-S$ ) anomalies along isopycnals (figure 4a). Denser than  $26.6 \text{ kg m}^{-3}$ , the deep water masses found offshore are largely homogenous. In the lighter water masses, there are

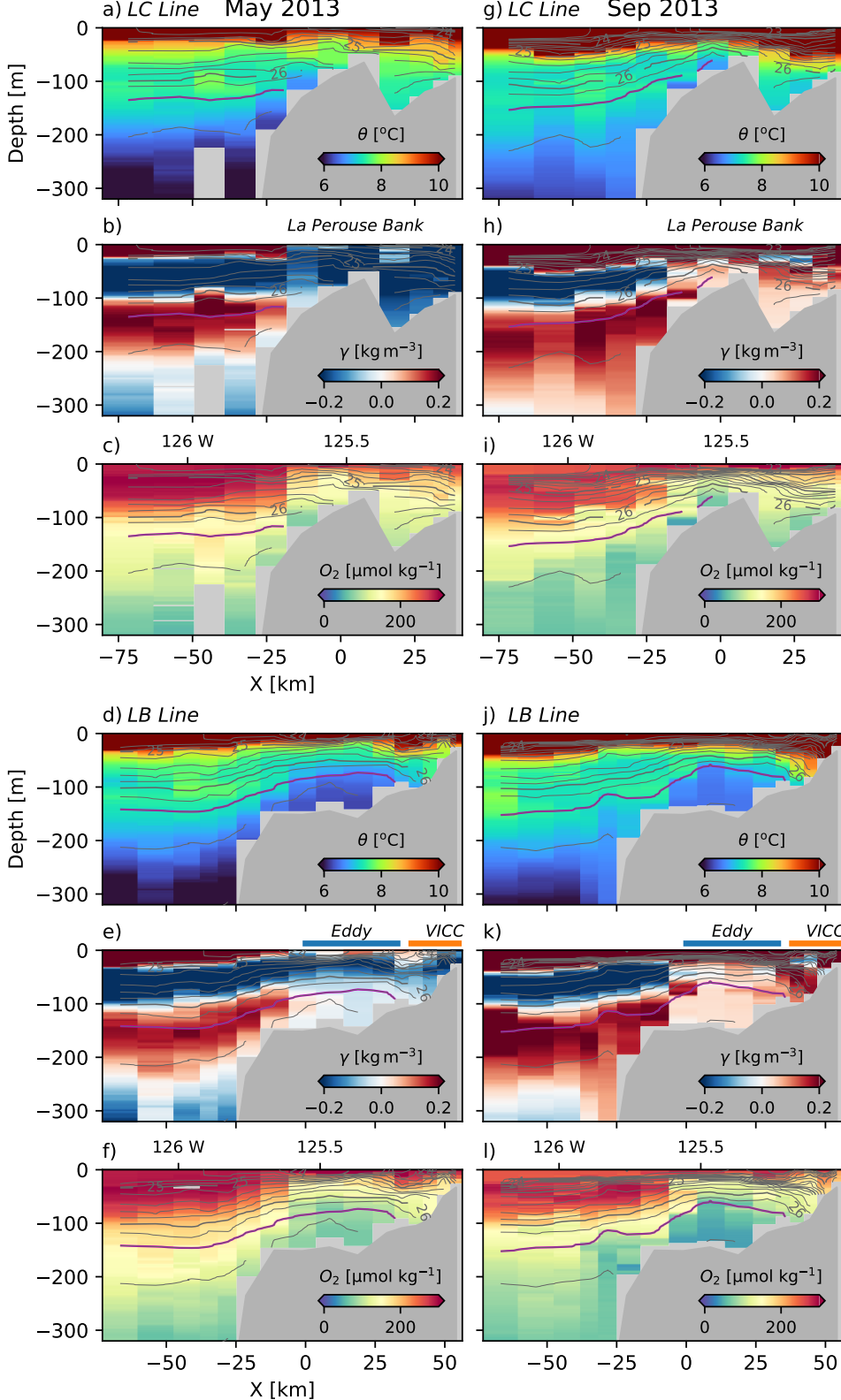


**Figure 3.** Observations along LC Line in May (a–c) and Sep (g–i) and LB lines in May (d–f) and Sep (j–l). X is across-shelf distance in the coordinate system shown in figure 1. Potential density is contoured every  $0.2 \text{ kg m}^{-3}$ , with the  $26.4 \text{ kg m}^{-3}$  colored magenta. Potential temperature,  $\theta$ , salinity anomaly,  $\gamma$  and oxygen concentration,  $O_2$ , are colored for each section.

174 distinct differences between warm and salty offshore water compared to water on the shelf  
175 at the same densities.

176 We use a spice anomaly defined as relative to a straight line in  $\theta$ - $S$  space (figure 4)  
177 representing an approximate mixing line for water in the EDDY, and passing through the  
178 points 7.75 °C, 30 psu and 6.6 °C, 35 psu. Spice anomaly for a given water sample at  
179 density  $\sigma_\theta$  is given by  $\gamma = \alpha(T - T_0(\sigma_\theta)) + \beta(S - S_0(\sigma_\theta))$  where  $T_0(\sigma_\theta)$ , where  $S_0(\sigma_\theta)$  are  
180 the temperature and salinity along the mixing line at the same density as the water sample.  
181 The sign convention is that a positive anomaly is warmer and saltier than data along the  
182 mixing line.

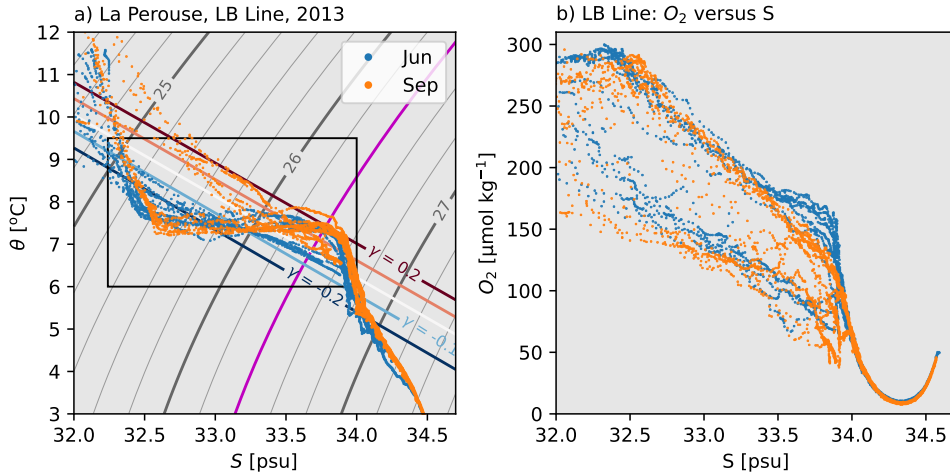


**Figure 4.** a) Potential temperature,  $\theta$ , versus salinity,  $S$ , for the La Perouse data shown in figure 3; potential density is contoured every  $0.2 \text{ kg m}^{-3}$ , with the  $26.4 \text{ kg m}^{-3}$  colored magenta. A definition of spice anomaly is shown in this plot, and discussed in the text. The rectangle is the  $\theta$  –  $S$  range used in figure 5 below. b) The same data with oxygen concentration versus salinity.

183 Using this metric of spice anomaly, offshore water tends to have high absolute values  
184 (figure 3, middle rows), with a positive-anomaly layer (red) centered at  $26.4 \text{ kg m}^{-3}$  sand-  
185 wiched between negative-anomaly layers above and below. On the shelf ( $-10 \text{ km} < X <$   
186  $30 \text{ km}$ ), the distinct  $\theta$ - $S$  masses are attenuated and much closer to the defined mixing line  
187 than the offshore water (closer to white in color in figure 3).

188 There are temporal changes over the summer. Away from the surface, water has  
189 upwelled from deeper depths by September, but the offshore water maintains the same water  
190 mass characteristics through the summer. Hugging the coast ( $X > 30 \text{ km}$ ), the Vancouver  
191 Island Coastal Current warms during the summer, and the spice anomaly goes from negative  
192 to positive. In the EDDY, the water stays near the mixing line, but is cooler in the spring  
193 (figure 3, LB Line, left-hand column: slightly negative spice anomaly) and warms during  
194 the summer (figure 3, LB Line, right-hand column: slightly positive spice anomaly).

195 Oxygen concentration in both surveys has a similar dichotomy between the EDDY and  
196 off-shelf water. Water found in the EDDY has oxygen concentrations  $100 \mu\text{mol kg}^{-1}$  lower on  
197 the shelf than off-shelf (figure 3, figure 4b). The very deepest water ( $S \approx 33.9 \text{ psu}$ ) on the  
198 shelf shows a further  $50 \mu\text{mol kg}^{-1}$  decrease in concentration between May and September  
199 along the LB line.

200            **3.2 Finescale surveys**

201            **3.2.1 Overview**

202            The finescale surveys covered most of the EDDY region, with an emphasis on the  
 203            offshore edge near the shelfbreak front (figure 1). For water denser than  $26 \text{ kg m}^{-3}$ , there  
 204            are three distinct water masses sampled on the shelf (figure 5). The first is offshore water,  
 205            which tends to be warmer, and hence has a positive spice anomaly ( $\gamma \approx 0.2 \text{ kg m}^{-3}$  along  
 206             $\sigma_\theta = 26.4 \text{ kg m}^{-3}$ ). The second is water in the EDDY, which during this survey was found  
 207            along the straight mixing line in  $\theta - S$  space (figure 5,  $\gamma \approx 0 \text{ kg m}^{-3}$  along  $\sigma_\theta = 26.4 \text{ kg m}^{-3}$ ).  
 208            Between these two water masses, there is a less populous mass (figure 5,  $\gamma \approx 0.1 \text{ kg m}^{-3}$   
 209            along  $\sigma_\theta = 26.4 \text{ kg m}^{-3}$ ) that we demonstrate below is found on the shelf poleward of the  
 210            EDDY.

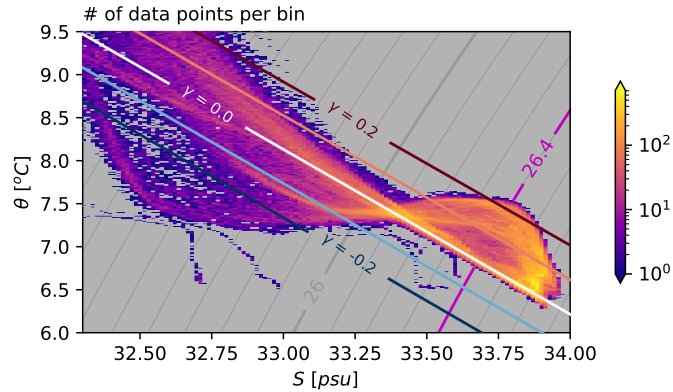


**Figure 5.** Binned sample density of salinity and potential temperature from the cruise, with a logarithmic color scale. Grey contours are potential density relative to the surface at intervals of  $0.1 \text{ kg m}^{-3}$ ; the magenta contour is the  $26.4 \text{ kg m}^{-3}$  isopycnal. Colored contours are spice anomaly,  $\gamma$ , relative to the white line labeled  $\gamma = 0.0$ .

211            In synthetic cross sections of spice anomaly, the EDDY is clearly identifiable as having  
 212            low spice anomaly ( $\gamma \approx 0 \text{ kg m}^{-3}$ , figure 6c, d). This signature of well-mixed water extends  
 213            from the seafloor to approximately 30 m depth, onshore of  $X \approx 0 \text{ km}$ . Despite lying along  
 214            a mixing line, the EDDY water is still stratified. The high-spice water ( $\gamma \approx 0.2 \text{ kg m}^{-3}$ )  
 215            is found offshore of the EDDY water, on the other side of a sharp  $\theta - S$  compensated  
 216            front. This front is even sharper in individual sections than in these composite sections (see  
 217            section 3.2.3).

218            In contrast, the third population of partially mixed water between the EDDY and  
 219            offshore water (figure 5) is all found poleward of the EDDY region (figure 6a, b) as water  
 220            with a weaker spice anomaly ( $\gamma \approx 0.1 \text{ kg m}^{-3}$ , pink colors). This water is not as warm as  
 221            offshore water, indicating some mixing with offshore water has taken place. Of note is that  
 222            this intermediate water mass appears completely absent in the sections further equatorward  
 223            (figure 6c, d), indicating that it is either mixed away or that it is advected elsewhere; we  
 224            argue below that it is advected offshore in a large-scale tongue.

225            Oxygen saturation sections show that the deep water in the EDDY has very low oxygen  
 226            saturation (figure 7c, d) compared to surrounding water (though again, we caution against  
 227            the quality of these saturation values from such a fast profiling instrument with a slow  
 228            response time). More oxygenated water is found offshore, and the oxygen deficit is not as  
 229            strong in the poleward sections (figure 7a, b). The T/S compensated front also shows an

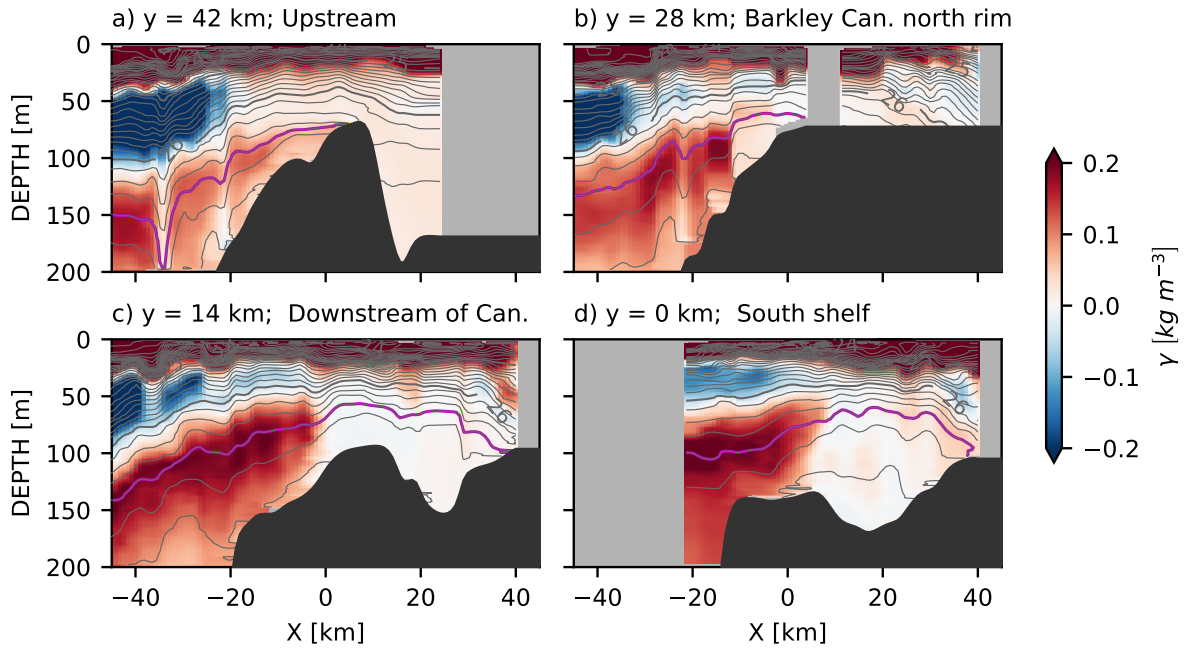


**Figure 6.** Synthetic sections of spice anomaly from the MVP data, projected along four lines from poleward (upstream of coastal current) a) to equatorward (downstream); the lines are shown in figure 1b). Isopycnals are contoured every  $\sigma_\theta = 0.2 \text{ kg m}^{-3}$ , with the  $\sigma_\theta = 26.4 \text{ kg m}^{-3}$  isopycnal highlighted in magenta. Colors are spice anomaly as defined in figure 5. "BC" in panel (c) refers to Barkley Canyon.

230 abrupt transition from the EDDY water and the offshore. Note the excellent correlation  
 231 between oxygen saturation and spice anomaly in figure 6.

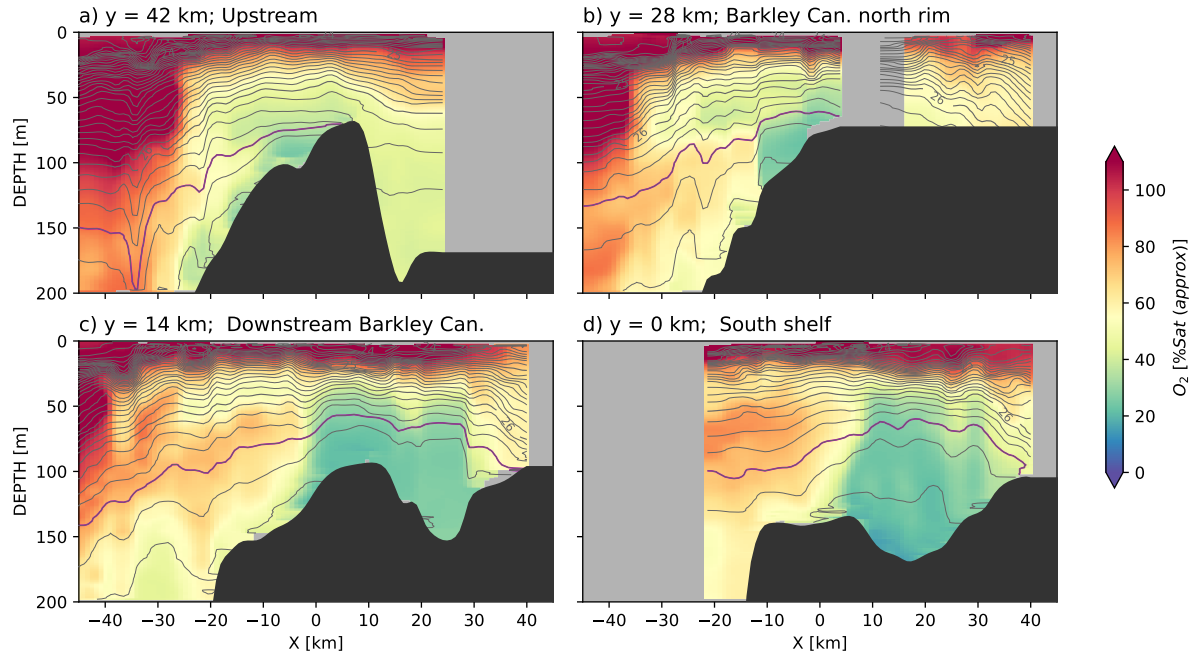


**Figure 7.** As in figure 6, for oxygen approximate saturation.

232 The spatial patterns are very clear when considering a map view of properties along  
 233 the  $\sigma_\theta = 26.4 \text{ kg m}^{-3}$  isopycnal (figure 8). There is a region onshore of the south tip of La  
 234 Perouse Bank (approximately  $44.5^\circ\text{N}$ ,  $125.75^\circ\text{W}$ ), that consists of water that is found along  
 235 the mixing line (spice anomaly  $\gamma \approx 0 \text{ kg m}^{-3}$ ) that also has low oxygen saturation. Offshore  
 236 of this region is water that is very warm and salty in comparison ( $\gamma > 0.15 \text{ kg m}^{-3}$ ), and  
 237 relatively high in oxygen (saturation of approximately 60%). The region between these two  
 238 water masses is very abrupt, and stretches from La Perouse Bank to a shallow bank just  
 239 above the Juan de Fuca canyon ( $48.3^\circ\text{N}$  and  $125.4^\circ\text{W}$ ).

240 Poleward of La Perouse bank and Barkley Canyon, the water along the shelf has the  
 241 weaker spice anomaly characteristic of the third water mass ( $\gamma \approx 0.1 \text{ kg m}^{-3}$ , light pink  
 242 colors). This water is also somewhat lower in oxygen than water from offshore, though  
 243 not as depleted as the water in the EDDY. This water appears to be pushed offshore just  
 244 upstream of Barkley Canyon and replaced on the shelf by the warmer (high spice) offshore  
 245 water.

### 246 3.2.2 Spur Canyon

247 The Spur Canyon leading from the Strait of Juan de Fuca has been implicated in  
 248 allowing dense water to be upwelled into the EDDY. The sea surface is low in the middle  
 249 of the EDDY, so it has been hypothesized that water moves up the Spur Canyon due to  
 250 ageostrophic motion (Weaver & Hsieh, 1987; Freeland & Denman, 1982). This is difficult  
 251 to infer from the observations collected here. Three transects up the canyon indicate that  
 252 deep isopycnals slope up into the canyon (figure 9, to approximately 30 km). Continuing  
 253 across the EDDY, isopycnals are largely flat until they intersect the Vancouver Island Coastal  
 254 Current (80 km). The deeper isopycnals are not found in the deeper basin northeast of La  
 255 Perouse bank (70 km), thus the bank is a natural poleward boundary of the EDDY.

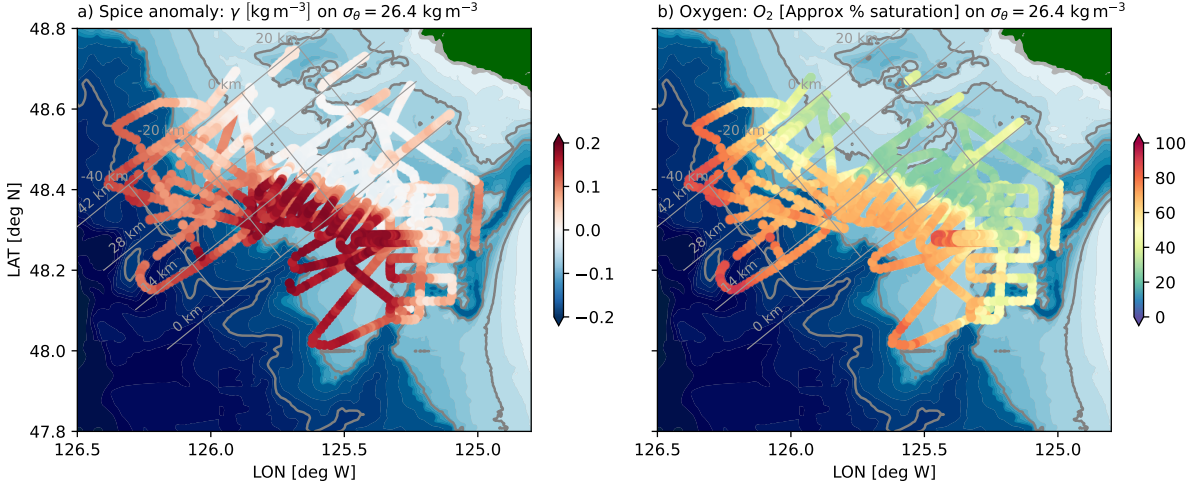


**Figure 8.** Spatial overview of a) the spice anomaly, and b) oxygen saturation on the  $\sigma_\theta = 26.4$  kg m<sup>-3</sup> isopycnal. Grey cross-slope lines are cross sections indicated in figure 6. Along-slope grey lines are every 20 km in the cross-slope direction, with  $X = 0$  km near the 100-m isobath at the north end of the observation area.

Spice anomaly along the canyon indicates a transition from offshore water to EDDY water. Oxygen saturation behaves in a similar manner, though some of the incoming water has slightly lower oxygen than water inside the EDDY (not shown). Based on these sections, it is difficult to infer water motion up the canyon.

Much of the modified water in the Spur Canyon appears to come from the shelf to the west, but heavily modified by tidal mixing. A repeat tidal survey over the bank on the west side of the canyon shows a strong hydraulic response during onshore flow (17:58–21:00, figure 10). Dense water passes from the offshore side into the canyon, and plunges down the side wall before rebounding downstream. Note that the tide here is largely diurnal, so this onslope flow only occurs once a day. Given the stratification of  $N \approx 6 \times 10^{-3}$  rad s<sup>-1</sup> and an overturning scale of 50 m, we might expect dissipation rates reaching  $\epsilon \sim L^2 N^3 \approx 5 \times 10^{-4}$  m<sup>2</sup> s<sup>-3</sup>, which is three orders of magnitude higher than dissipation observed on the shelf west of this location by Dewey and Crawford (1988). This estimate of turbulence dissipation rate implies a diapycnal diffusivity of  $\kappa = \gamma \epsilon / N^2 \approx 1$  m<sup>2</sup> s<sup>-1</sup>, assuming a mixing efficiency of  $\gamma = 0.2$ . Water spills over from the offshore front into the canyon during the onshore tide. This water is rapidly mixed with surrounding water such that its strong offshore spice values are attenuated.

The turbulence found on the canyon rim makes it ambiguous if there is water moving up the canyon or not. There is a general tendency along the canyon for higher spice water to be found offshore (figure 9) but it seems likely that the source of the higher spice water is from over the bank rather than water being advected up the canyon. This tidally driven flow over the bank is the most significant source of high-spice offshore water into the eddy region identified during our surveys.

### 3.2.3 Frontal survey

A systematic survey through the front between the offshore water and the EDDY water demonstrates the sharpness and persistence of this front (figure 11), suggesting that it has limited exchange with the offshore region.

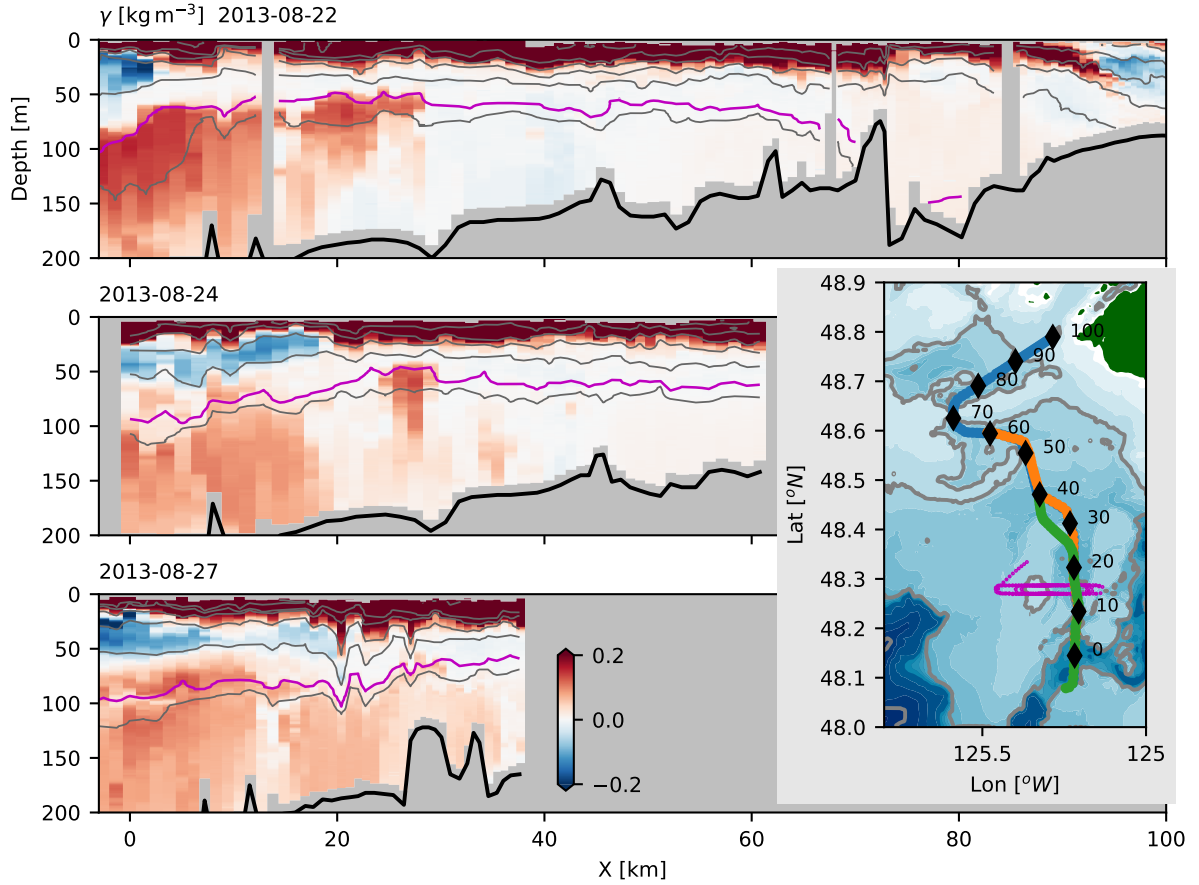


**Figure 9.** Spice anomaly surveys up the Spur Canyon, where  $X$  is along-canyon as defined in the map. Grey isopycnals are contoured every  $0.5 \text{ kg m}^{-3}$ , and the  $26.4 \text{ kg m}^{-3}$  isopycnal is shown in magenta. The seafloor is indicated with the thick black line. Map (lower right) shows the path taken during each survey in chronological order (blue, orange, and green). Magenta line is path taken during a cross-canyon survey (figure 10).

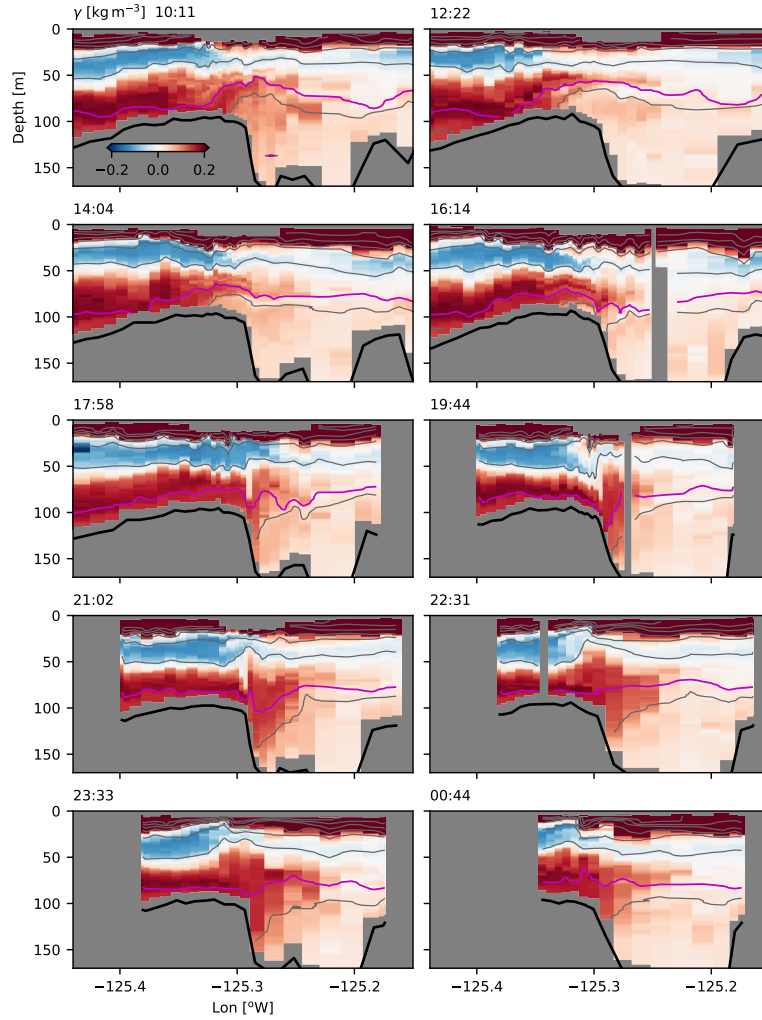


**Figure 10.** Spice anomaly observed in repeated, tide-resolving survey across the Spur Canyon, time is indicated in the upper left of each plot (29 August, 2013). Location of survey shown in figure 9 as a magenta line.

283        The survey started close to shore, and passed through the Vancouver Island Coastal  
 284        Current (along-track 0-10 km). The coastal current forms a buoyant front, and is fresher  
 285        and colder than water at the same density. This front is relatively thick, greater than 20  
 286        km wide, and has partially mixed water from the surface to the foot of the front ( $\gamma \approx 0.1$ ).

287        Offshore of this coastal current, measurements were collected crossing the front be-  
 288        tween the offshore water and the EDDY water 10 times, showing its evolution following the  
 289        along-shore equatorward flow. First, as noted in the composite sections, isopycnals slope up  
 290        from offshore onto the shelf. In the first crossing, the front is very sharp, (along-track dis-  
 291        tance 50 km) though two small tendrils can be seen separating from the front on the inshore  
 292        side. Similar tendrils are found on the second crossing, perhaps a bit more separated from  
 293        the front ( $\approx 80$  km), and on the third crossing ( $\approx 95$  km). These tendrils are made of up  
 294        partially mixed water. The subsequent passes have more of this partially mixed water, such  
 295        that the partially mixed front is up to 5-km wide by the fifth pass ( $\approx 150$  km). However,  
 296        the deeper isopycnals retain a sharp front, and indeed the front appears sharp again by the  
 297        seventh pass at all depths ( $\approx 200$  km).

298        There is evidence of some warmer water swirling into Eddy, particularly along isopy-  
 299        cnals deeper than  $26.4 \text{ kg m}^{-3}$ . Regions of warmer (and more oxygenated) water are found  
 300        in tendrils at these depths (e.g.  $\approx 170$  km and  $\approx 185$  km). The overall effect is similar to  
 301        what was seen in the Gulf Stream with similar observations (Klymak et al., 2016); there  
 302        are two quite distinct water masses, the Eddy water and the offshore water, as seen in the  
 303         $\theta$ - $S$  plot (figure 11c) with only a small population of samples between these two. This  
 304        distribution of  $\theta$ - $S$  properties is indicative of substantial isopycnal and vertical mixing, but  
 305        even these populations are relatively cut off from the main water masses, indicating that  
 306        they are well-mixed on their own, in short episodic events. Regardless, this front is very  
 307        sharp given that it has no density signature, indicating that there is not strong advection  
 308        from offshore into the EDDY region.

### 309        3.3 Separation of coastal water

310        Upstream of the the sharp front between the low-spice EDDY and the high-spice off-  
 311        shore water is a substantial mass of intermediate-spice water along the shelf (compare figure  
 312        6a and c). This intermediate spice water is moving equatorward along the shelf upstream  
 313        of the EDDY, but is pushed offshore just upstream of Barkley Canyon (figure 12). There is  
 314        a tongue of intermediate-spice water ( $\gamma$  is pink along  $26.4 \text{ kg m}^{-3}$ ) that separates from the  
 315        shelf just west of  $126^{\circ}\text{W}$ . The surveys do not cross the full extent of the tongue, but it is  
 316        at least 30 km wide. It also appears to end at approximately  $48.2^{\circ}\text{N}$ . This intermediate-  
 317        spice water reaches from relatively shallow isopycnals to at least  $26.6 \text{ kg m}^{-3}$  (figure 12, left  
 318        panel). Unfortunately, we cannot track the fate of this water mass because isopycnals tilt  
 319        down offshore, below the depth limit of the MVP. The  $25.5 \text{ kg m}^{-3}$  isopycnal appears to have  
 320        the tongue closer to the shelf than at  $26.4 \text{ kg m}^{-3}$ , indicating strong three-dimensionality to  
 321        this feature.

322        This separating tongue is embedded in the larger scale isopycnal tilt caused by the  
 323        upwelling (figure 12, right panels), so it is difficult to see dynamically what is driving this  
 324        offshore push. One possibility is that it is simple flow separation caused by the water not  
 325        being able to make the sharp turn around La Perouse Bank. Whatever causes it, downstream  
 326        of the separation, the water is replaced by offshore water with much higher spice values.

327        There is a clear surface expression of the separating tongue in satellite imagery (fig-  
 328        ure 13). Water flowing equatorward along the shelf tends to be cooler than offshore water,  
 329        likely due to mixing with the colder coming out of the Strait of Juan de Fuca. On August  
 330        25, there is a cold tongue of water separating from La Perouse bank, crossing isobaths and  
 331        pointing south at  $125.8^{\circ}\text{W}$ . There is a cooler tendril streaming west at  $48^{\circ}\text{N}$  off the south end  
 332        of this tongue. This feature is not as well-developed in the previous image (Aug. 21) perhaps  
 333        indicating that it is an evolving feature. By 31 August, there is no surface expression of

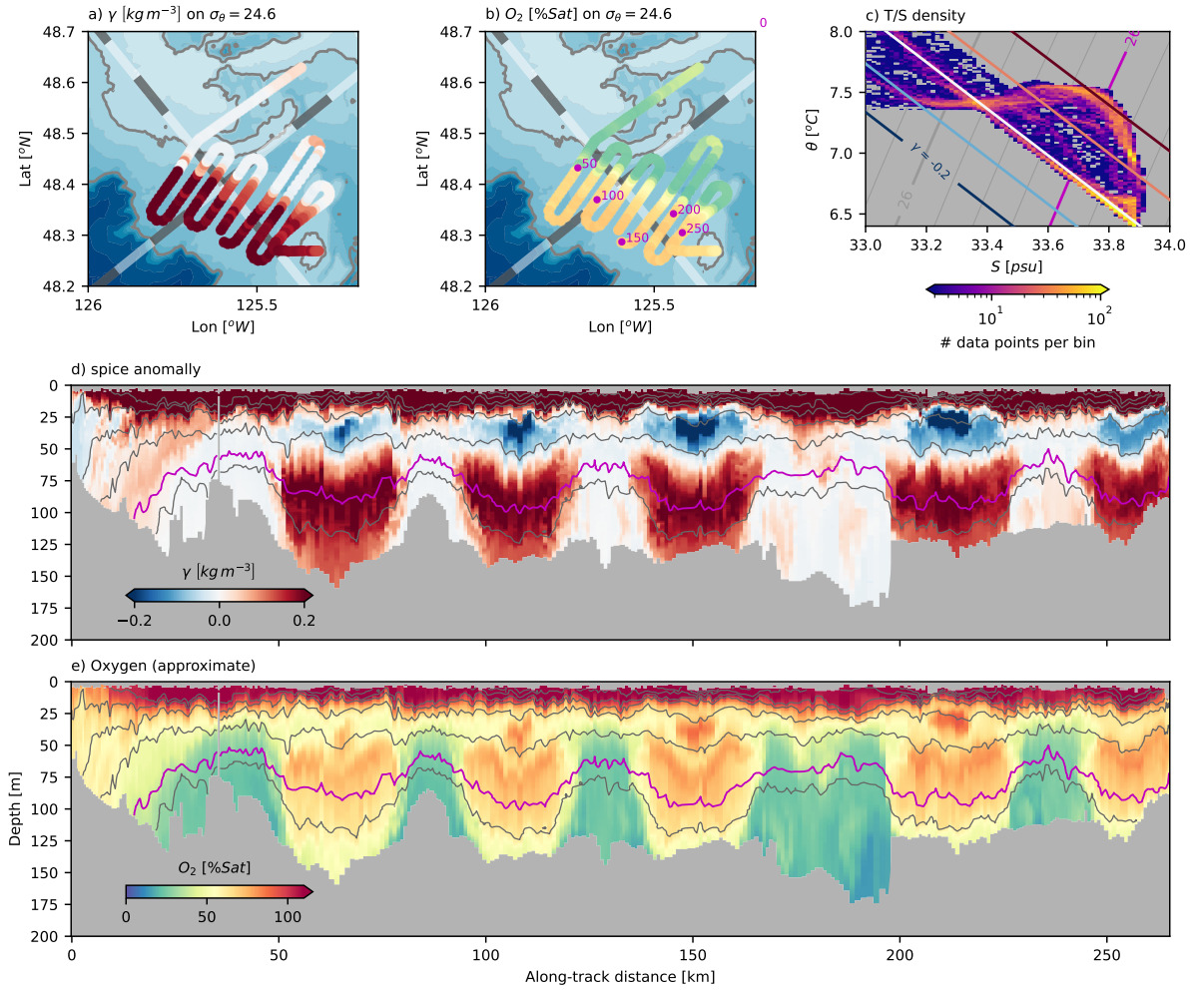


**Figure 11.** Data from the frontal survey a) spice anomaly along  $26.4 \text{ kg m}^{-3}$ . Grey-white alternating lines are the coordinate system, with 10-km alternating shades. b) oxygen saturation along  $26.4 \text{ kg m}^{-3}$ ; magenta dots correspond to distance along-track. c) density of data points (logscale) in this section of data. d) cross-section of spice anomaly along track. Grey isopycnals are contoured every  $0.5 \text{ kg m}^{-3}$ , and the  $26.4 \text{ kg m}^{-3}$  isopycnal is shown in magenta. e) cross-section of oxygen saturation.

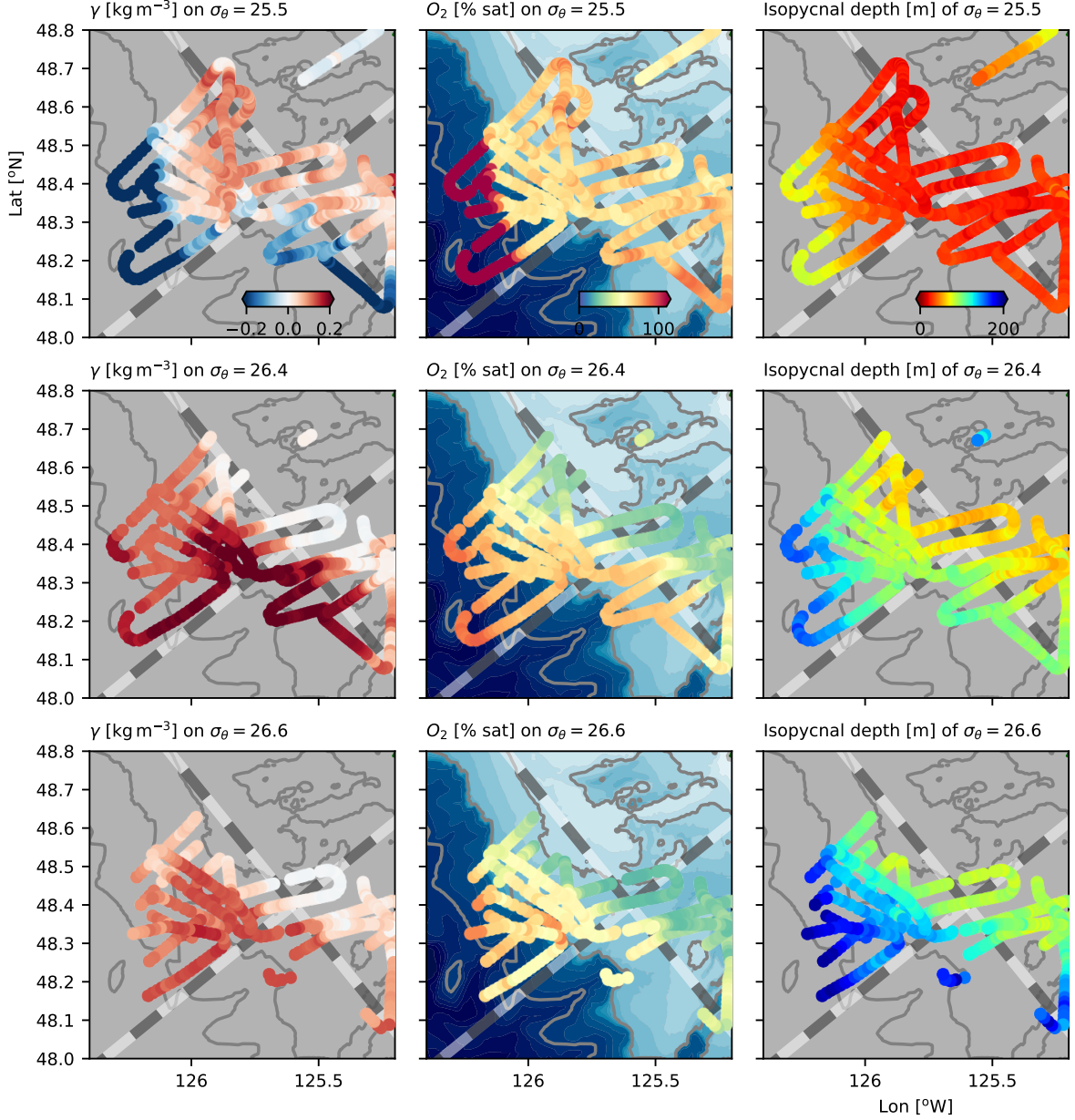


**Figure 12.** Isopycnal slices through showing the vertical structure of the water separating from the shelf, with the first row along  $25.5 \text{ kg m}^{-3}$ , second along  $26.4 \text{ kg m}^{-3}$ , and the third at  $26.6 \text{ kg m}^{-3}$ . First column is the spice anomaly, second is oxygen saturation, and the last column is depth of each isopycnal.

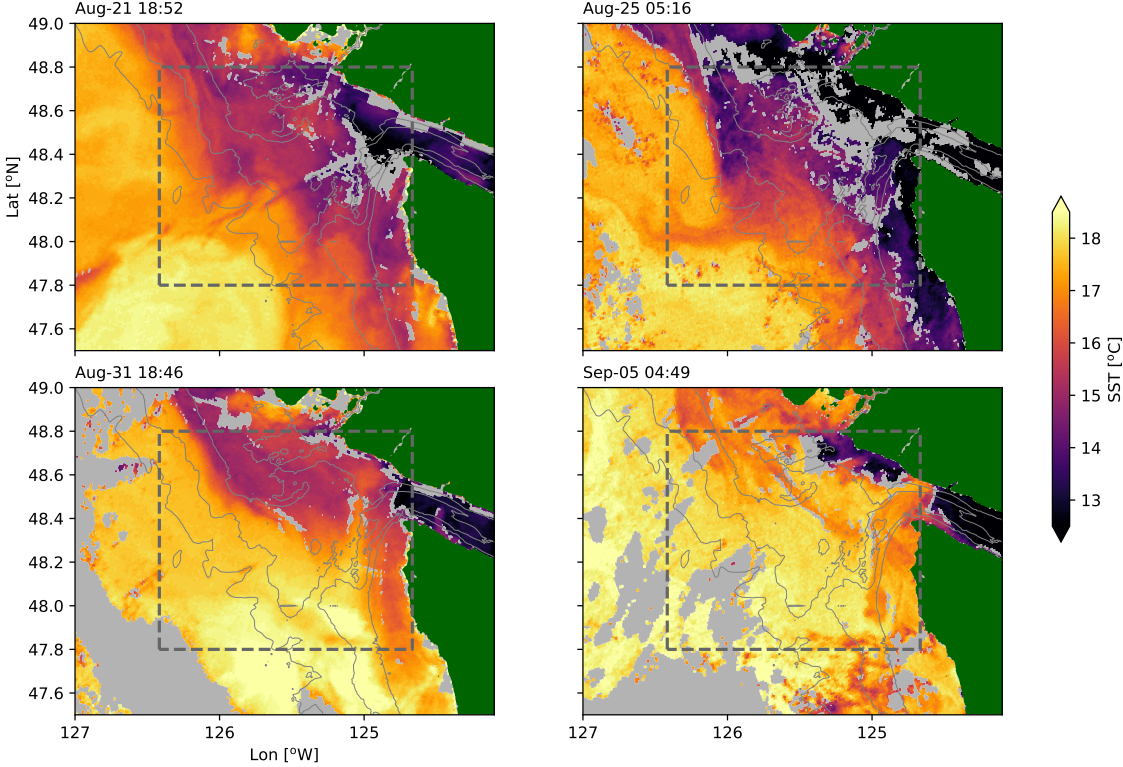


**Figure 13.** Sea surface temperature snapshots from the observation period. Grey areas are clouds; dashed gray line is the study area. Depths are contoured in thin gray lines at 200, 150 and 100 m. (OSI SAF, 2015)

the feature, though small tendrils of cooler water can be seen separating from La Perouse Bank. By 5 September, the water has significantly warmed, and the offshore anomaly does not appear to have a surface signature.

Satellite-based surface chlorophyll estimates show the same feature (figure 14) demonstrating the advection of high chlorophyll to the west side of the EDDY. They also show a relatively high-chlorophyll tendril to the west, again exiting the study region at approximately 48 degrees N. The feature is relatively long-lived, on the order of one month. Inspection of images before August 5 were too obscured by clouds or did not show this feature. By September 6, we see the feature fading from the satellite image. Note that this feature is centered 0.2 degrees of latitude south of tongue that we observe deeper in the water column, again indicating that there is depth-dependent structure in the feature.

#### 4 Summary and Discussion

The intensive sampling discussed here has demonstrated a few important features of the South Vancouver Island Shelf. The Juan de Fuca Eddy water is readily identified as falling along a mixing line in  $\theta - S$  space, compared with offshore water that was warmer and saltier (high-salinity anomaly). There was not strong evidence of the EDDY being supplied by water moving up the Spur Canyon during our observations, but the Spur Canyon was a site of hydraulic cross-canyon flows in which we infer significant mixing. There is a sharp and persistent temperature-salinity compensated front between offshore water and the partially mixed EDDY water. Finally, upstream of the EDDY, water in the equatorward shelf current

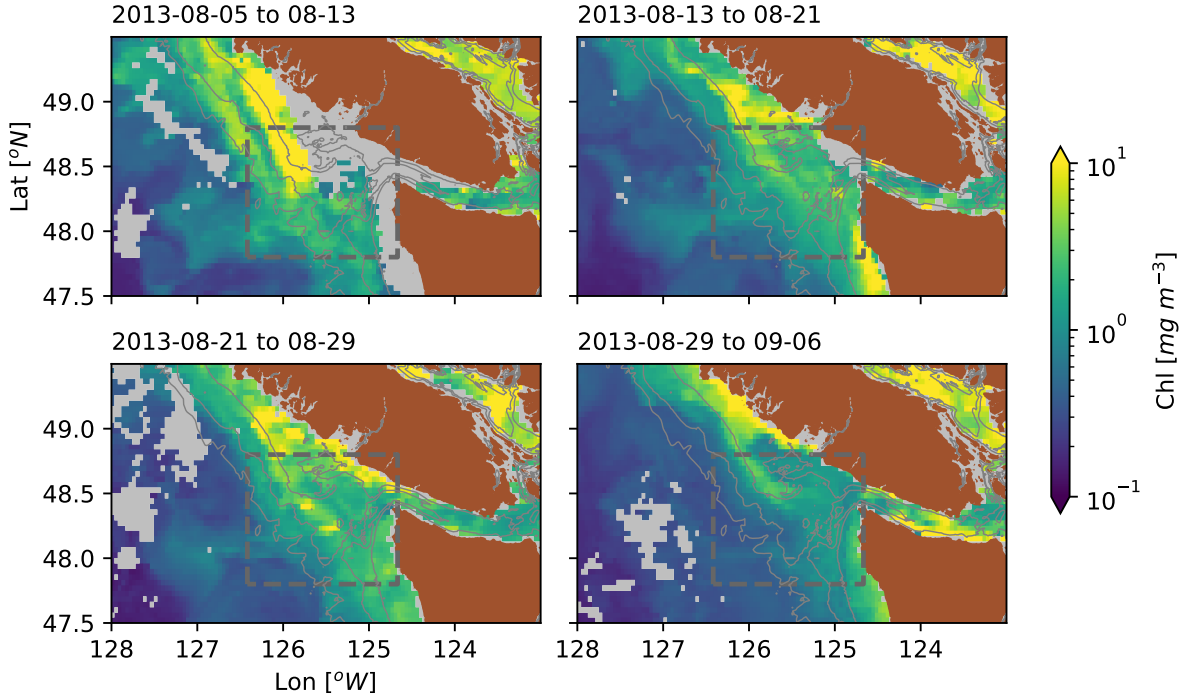


**Figure 14.** Surface chlorophyll density estimated from ocean color (Hu et al., 2012; NASA Ocean Biology Processing Group, 2017) over 8-day windows in 4-km bins. Gray regions had too many clouds to compute averages.

has intermediate spice anomaly, and is seen to separate from the shelf at the point of an abrupt bend in an underwater bank. The water mass crosses isobaths and is ejected into the interior. This separation event can also be observed from satellite measurements of sea surface temperature and chlorophyll. Thus the water that is offshore of the EDDY appears to have been brought onto the shelf in exchange for the offshore ejection of shelf water via this tongue.

#### 4.1 Age and source of the EDDY water

The source of water and formation mechanism of the Juan de Fuca Eddy has received substantial attention, however, the observations of EDDY waters being found along a tight mixing line in  $\theta$ - $S$  space has not previously been noted. The deepest water in the EDDY could originate along the  $\theta$ - $S$  line from approximately 5.5°C to 7.5°C (figure 4a), which in the open ocean spans depths from 420 m to 70 m. Mackas et al. (1987) attempted to determine the origin of the water by including oxygen as a third variable to resolve the ambiguous  $\theta$ - $S$  relation. However, as figure 4b makes clear, oxygen does not appear to be a conserved property in the EDDY, with concentrations up to 150  $\mu\text{mol kg}^{-1}$  lower in the EDDY than the water found offshore, and in a way that definitely cannot be the result of conservative mixing. As a best guess, if the water in the deepest part of the EDDY came from a vertical mixture of the water at  $26.5 \text{ kg m}^{-3}$  and an equal distance down in density space of  $26.7 \text{ kg m}^{-3}$ , then the deepest water in the EDDY may be coming from a depth of 250 m. This is a typical upwelling depth for coastal flows, and may not require extra input up the Spur Canyon as posited by Freeland and Denman (1982).

375 We found little evidence of flow up the Spur Canyon or, if there is, then the mixing in  
 376 the canyon is intense enough to remove the  $\theta$ - $S$  signature of offshore water within 20 km of  
 377 the canyon mouth (figure 9). We did find substantial evidence of mixing in the canyon, but  
 378 the primary pathway of high-salinity water into the canyon appears to be due to tidal flow  
 379 over the banks on the west side (figure 10), rather than flow up the canyon. However, it is  
 380 worthy of note that upwelling winds had ceased at the point of these observations (figure 2),  
 381 so the offshore surface pressure gradient may be reduced, leading to reduced ageostrophic  
 382 upwelling in the canyon. Whether the cessation of winds would also lead to a reduction of  
 383 the low sea level height in the center of the EDDY that may drive up-canyon flow is an open  
 384 question.

385 There is evidence of aging of the water in the EDDY between late spring and late  
 386 summer (figure 3), with a reduction of oxygen in the EDDY over this time span. If we  
 387 posited that the reduction was all in the same water, then the oxygen consumption rate  
 388 over the time between the late-May and early September cruises would be on the order of  
 389  $0.5 \mu\text{mol kg}^{-1}\text{d}^{-1}$ . This is on the low side of estimates of apparent oxygen utilization rates  
 390 in continental upwelling systems, which are between 1 and  $5 \mu\text{mol kg}^{-1}\text{d}^{-1}$  (Dortch et al.,  
 391 1994). So it seems possible the EDDY had enough exchange with the surrounding water for  
 392 the residence time to have been less than the full time period from late May to September.  
 393 Note that during the May cruise, the water in the EDDY is slightly cooler than the mixing  
 394 line, and during the September cruise is slightly warmer than the mixing line, so the water  
 395 in the EDDY is evolving seasonally, and probably affected by the water temperature in the  
 396 Vancouver Island Coastal Current and the amount of water getting through the onshore  
 397 front.

398 The water is mixed enough in the EDDY that it falls along a mixing line, though it  
 399 remains vertically stratified. The amount of homogenization is such that either the mixing is  
 400 very strong, or the water is retained in the EDDY for a long time. The amount of turbulence  
 401 required to homogenize 100 m of water over 90 days is  $\kappa \approx 10^{-3} \text{ m}^2\text{s}^{-1}$ . Given that the  
 402 diffusivity implied in the cross-channel surveys was on the order of  $\kappa_\rho = 10 \text{ m}^2\text{s}^{-1}$ , this  
 403 number is not outrageous if we think that such high dissipation is found in  $10^{-4}$  of the  
 404 water column. We can more carefully quantify this by considering a synthetic profile or  
 405 temperature and salinity based on an offshore profile, extrapolated from the bottom of the  
 406 200-m cast to 250 m, assuming that the temperature and salinity at 250 m are  $6.2 [\text{°C}]$  and  
 407 34 psu respectively (figure 15). Water at the offshore station was warmer than onshore, so  
 408 the profile was also linearly interpolated to a surface value of ( $12 \text{ °C}$ , 31.6 psu). The profile  
 409 was then linearly compressed into a depth range of 150 m representative of the shelf depth in  
 410 the dense pool, and subjected to mixing with a constant diffusivity of  $\kappa = 10^{-3} \text{ m}^2\text{s}^{-1}$ , with  
 411 the surface and bottom values pinned under the assumption that the near-bottom source  
 412 and surface waters are replenished from a large reservoir. Similar to the naive scaling, the  
 413 T-S relationship does not approach a straight line until after approximately 60-100 days, or  
 414 until the mixing affects a vertical length scale of  $\lambda = (\tau\kappa)^{1/2}$  that is greater than  $\approx 70 \text{ m}$ .

415 The sharpness of the front with the EDDY and the offshore water is intriguing. It was  
 416 persistent for the duration of our detailed survey (figure 8), and, so far as we can tell with  
 417 the limited resolution of the hydrographic surveys, was present during the bracketing La  
 418 Perouse cruises. There is not any substantial bathymetry blocking the onshore incursion of  
 419 water at this location, so there must be a dynamic barrier.

420 Numerical simulations of this region reported by (Sahu et al., 2022) using a NEMO  
 421 36th-degree regional model contained relatively rapid exchange between the deep EDDY  
 422 water and the rest of the coastal ocean. The region where the EDDY resides has velocities  
 423 equal or greater than other parts of the shelf, and water has an approximate residence time  
 424 of less than 20 days. The EDDY water in the model does develop a distinct  $\theta$ - $S$  signature,  
 425 but not along a sharp mixing line as observed. It also has a front with the offshore water,  
 426 but the front is substantially wider than that observed here.

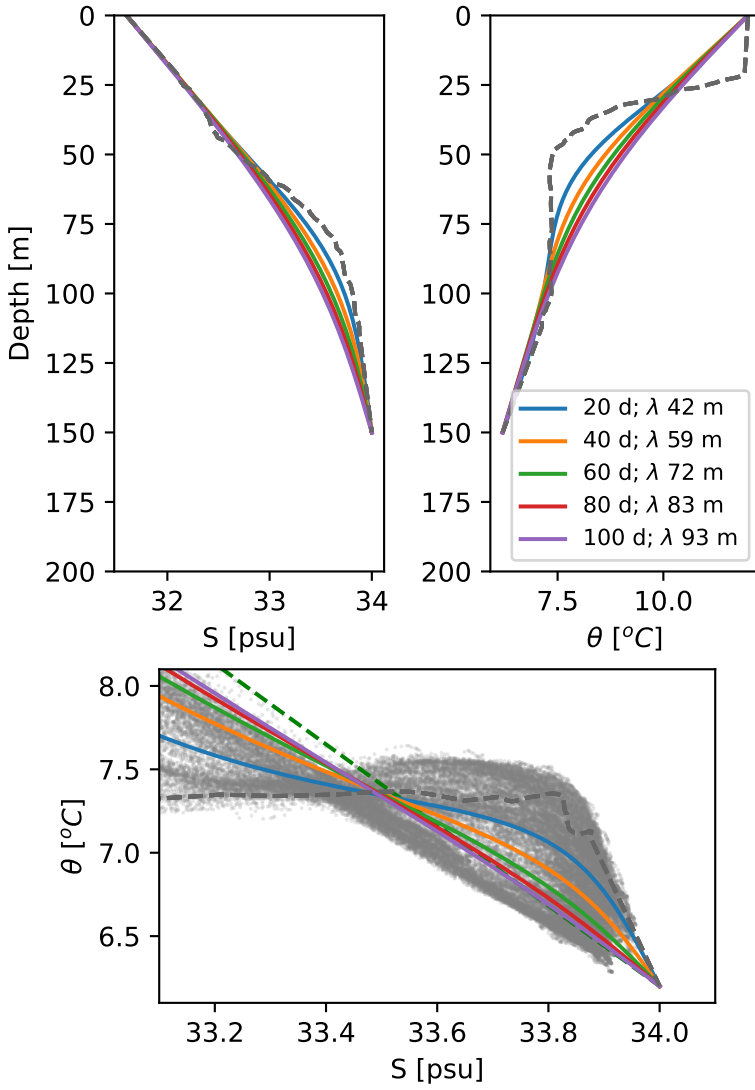


**Figure 15.** Mixing model assuming constant eddy diffusivity of  $\kappa = 10^{-3} \text{ m}^2 \text{s}^{-1}$  acting on an offshore temperature and salinity profiles compressed from 250 thick to 150 m thick (grey dashed lines). Profiles are pinned to the deep  $\theta - S$  value at (34 psu, 6.2 °C), and a shallow one at (31.6 psu, 12 °C). The green dashed line is the mixing line defined in the text.

427 Overall, it would be an improvement to our understanding of the EDDY if we could  
 428 sample the shelf more persistently. The EDDY was already well-formed by the May La  
 429 Perouse cruise, and seems to evolve slowly during that time. Capturing its formation,  
 430 presumably earlier in the spring, as well as its evolution through the year, would be valuable  
 431 in understanding retention and exchange on this productive part of the shelf.

#### 432 4.2 Offshore exchange of shelf water

433 The displacement of shelf water from La Perouse Bank is a dramatic departure from  
 434 geostrophically balanced isobath-following flow. Eddies have been known to separate from  
 435 irregular coastal topography, both at the surface (Barth et al., 2000) and deeper in the  
 436 water column (Pelland et al., 2013). It has been recognized that instabilities lead to exchange  
 437 between the open ocean and the shelf at this location (Ikeda & Emery, 1984, 1984). However,  
 438 observations of the wholesale replacement of shelf water by a new water mass from offshore  
 439 are rare. In the observations presented here, it is clear that water from as deep as 150 m is  
 440 separating from the shelf and moving offshore (figure 8, figure 12).

441 Satellite imagery shows that there is often exchange between coastal and deep waters  
 442 along the Vancouver Island shelf (figure 16). Most years there are three of four large filaments  
 443 from the shelf into the open ocean, many of them over 100 km long. This length scale is  
 444 longer than the 60 km inferred for this region by Ikeda et al. (1984) using a four-layer  
 445 instability analysis. It is possible that there is spatial locking of these features, with a  
 446 persistent separation at the north tip of Vancouver Island, and a strong tendency for one  
 447 at 49.5 N. There is also evidence of separation events in most of the years, with 2011  
 448 being the only clear exception. General baroclinic instability of the upwelling front is a  
 449 possible mechanism to drive offshore exchange (Ikeda et al., 1984; Durski & Allen, 2005),  
 450 but this tends to be shallow, with smaller-scale instabilities that will not extend as far into  
 451 the interior ocean as observed here. Rather it seems likely that the topographic change  
 452 engendered by the sudden turn to the east of La Perouse bank catalyses a larger scale  
 453 instability at this location. Durski and Allen (2005), when modelling the Oregon shelf,  
 454 found that including realistic shelf bathymetry catalyzed intermittent large-scale instabilities  
 455 similar to the feature here, a finding that is deemed likely to apply at other coastal locations  
 456 (Batteen, 1997).

457 Large-scale mixing between the shelf and open ocean has been evident since the satellite  
 458 era. Here we demonstrate that in the Vancouver Island shelf the flow is originating on the  
 459 shelf and separating from the bathymetry and being injected into the interior. A similar  
 460 observation was made by Barth et al. (2000) downstream of Cape Blanco, Oregon, where  
 461 the coastal current was observed to detach from the shelf in the lee of the cape and flow into  
 462 the interior. They hypothesized that as the current moved offshore, it deepened, stretching  
 463 isopycnals and creating cyclonic relative vorticity that would tend to push the current back  
 464 onshelf, but then it was caught in the undercurrent and stalled, being pushed offshore. It is  
 465 also possible that coastally trapped waves in the region experience a hydraulic control, and  
 466 these separation events are part of the response (Dale & Barth, 2001).

467 Regardless of the dynamics of the separation events, the offshore transport can be  
 468 substantial. If we assume the coastal current is approximately  $0.1 \text{ m s}^{-1}$  over 100 m in the  
 469 vertical and 20 km in the horizontal, it represents 0.2 Sv of nutrient- and chlorophyll-rich  
 470 shelf water transported offshore. Our observations are a finer detailed representation of the  
 471 kind of cross-shore transports inferred by Mackas and Yelland (1999) from hydrographic  
 472 surveys, and definitively show that this water can originate from the shelf from relatively  
 473 deep depths and be transported offshore. We do not have velocity measurements for the  
 474 water that replaces it, but assuming that water also flows along-shelf, these separation  
 475 events are associated with a large replacement of shelf water with offshore water at this  
 476 location. This emphasizes the importance of three dimensional observations and modeling  
 477 of cross-shelf dynamics when thinking about physical and biological processes on the shelf.

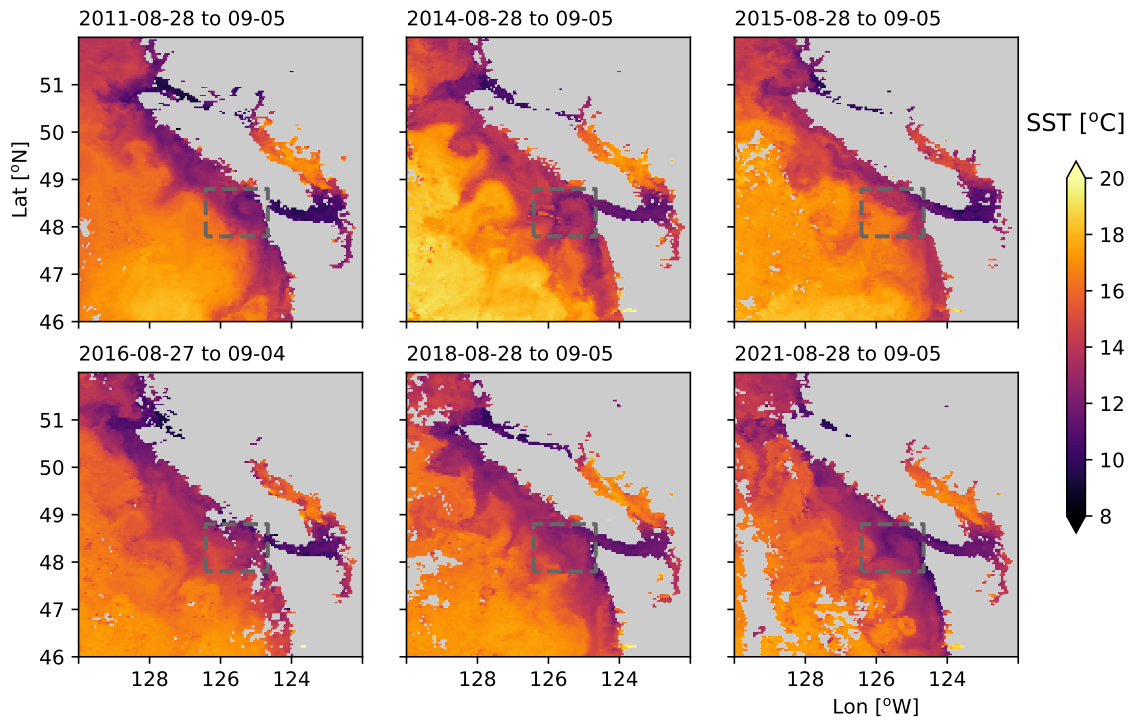


**Figure 16.** Available late-August sea-surface temperature from 8-day composites, 2011 to 2021 (NASA Ocean Biology Processing Group, 2019); missing years had too much cloud cover or no satellite coverage.

## 478 Open Research

479 Derived data files (1-m vertical binned CTD files) and analysis scripts are available at  
 480 <https://ocean-physics.seos.uvic.ca/~jklymak/PW13DataAnalysis/>. Raw CTD data  
 481 is available on request. Data was processed using a scientific python toolchain as listed at  
 482 <https://ocean-physics.seos.uvic.ca/~jklymak/PW13DataAnalysis/environment.yml>;  
 483 major components include xarray (Hoyer & Hamman, 2017), numpy (Harris et al., 2020),  
 484 and Matplotlib (Caswell et al., 2022), but those all leverage many smaller but vital projects.

## 485 Acknowledgments

486  
 487 Thank you to the officers and crew of the R/V Falkor and the Schmidt Foundation  
 488 for funding the seagoing component of the cruise. Thank you to Richard Dewey, Benjamin  
 489 Schieffe, and Rowan Fox for efforts during the cruise. Klymak was supported by NSERC  
 490 Discovery grant RGPIN-2017-04050 and a Canadian Foundation for Innovation Leading  
 491 Edge Fund grant 36109, Allen was supported by NSERC Discovery grant RGPIN-105694-  
 492 11, and Waterman was supported by NSERC Discovery grant RGPIN-2020-05799.

## 493 References

- 494 Barth, J. A., Pierce, S. D., & Smith, R. L. (2000). A separating coastal upwelling jet at  
 495 Cape Blanco, Oregon and its connection to the California Current system. *Deep Sea*  
 496 *Res. II*, 47(5–6), 783 - 810. doi: [http://dx.doi.org/10.1016/S0967-0645\(99\)00127-7](http://dx.doi.org/10.1016/S0967-0645(99)00127-7)
- 497 Batteen, M. L. (1997). Wind-forced modeling studies of currents, meanders, and eddies in  
 498 the California Current system. *J. Geophys. Res.*, 102(C1), 985–1010. doi: [10.1029/96jc02803](https://doi.org/10.1029/96jc02803)
- 500 Brink, K. (2016). Cross-shelf exchange. *Annu. Rev. Mar. Sci.*, 8(1), 59–78. doi: [10.1146/annurev-marine-010814-015717](https://doi.org/10.1146/annurev-marine-010814-015717)
- 501 Castelao, R. M., & Barth, J. A. (2007, nov). The role of wind stress curl in jet separation  
 502 at a cape. *J. Phys. Oceanogr.*, 37(11), 2652–2671. doi: [10.1175/2007jpo3679.1](https://doi.org/10.1175/2007jpo3679.1)
- 503 Caswell, T. A., Lee, A., Droettboom, M., De Andrade, E. S., Hoffmann, T., Klymak, J.,  
 504 ... Kniazev, N. (2022). *matplotlib/matplotlib: Rel: v3.6.0*. Zenodo. Retrieved from  
 505 <https://zenodo.org/record/7084615> doi: [10.5281/ZENODO.7084615](https://doi.org/10.5281/ZENODO.7084615)
- 506 Dale, A. C., & Barth, J. A. (2001, jan). The hydraulics of an evolving upwelling jet flowing  
 507 around a cape. *Journal of Physical Oceanography*, 31(1), 226–243. doi: [10.1175/1520-0485\(2001\)031<0226:thoaeu>2.0.co;2](https://doi.org/10.1175/1520-0485(2001)031<0226:thoaeu>2.0.co;2)
- 508 D'Asaro, E. (1988). Generation of submesoscale vortices: A new mechanism. *J. Geophys.*  
 509 *Res.*, 93, 6685–6693.
- 510 D'Asaro, E. A., Shcherbina, A. Y., Klymak, J. M., Molemaker, J., Novelli, G., Guigand,  
 511 C. M., ... Özgökmen, T. M. (2018, Jan). Ocean convergence and the dispersion of  
 512 flotsam. *Proc. Natl. Acad. Sci. U.S.A.*, 201718453. doi: [10.1073/pnas.1718453115](https://doi.org/10.1073/pnas.1718453115)
- 513 Dewey, R. K., & Crawford, W. R. (1988). Bottom stress estimates from vertical dissipation  
 514 rate profiles on the continental shelf. *J. Phys. Oceanogr.*, 18, 1167–1177.
- 515 DFO. (2022). *Marine environmental data section archive, buoy c46206*. Ecosystem and  
 516 Oceans Science, Department of Fisheries and Oceans Canada. Retrieved 2022-01-31,  
 517 from <https://meds-sdmm.dfo-mpo.gc.ca>
- 518 Dortch, Q., Rabalais, N. N., Turner, R. E., & Rowe, G. T. (1994, dec). Respiration rates  
 519 and hypoxia on the Louisiana shelf. *Estuaries*, 17(4), 862. doi: [10.2307/1352754](https://doi.org/10.2307/1352754)
- 520 Durski, S. M., & Allen, J. S. (2005). Finite-amplitude evolution of instabilities associated  
 521 with the coastal upwelling front. *J. Phys. Oceanogr.*, 35(9), 1606–1628. doi: [10.1175/jpo2762.1](https://doi.org/10.1175/jpo2762.1)
- 522 Engida, Z., Monahan, A., Ianson, D., & Thomson, R. E. (2016). Remote forcing of sub-  
 523 surface currents and temperatures near the northern limit of the California Current  
 524 system. *J. Geophys. Res.*, 121(10), 7244–7262. doi: [10.1002/2016jc011880](https://doi.org/10.1002/2016jc011880)

- 528 Foreman, M. G. G., Callendar, W., MacFadyen, A., Hickey, B. M., Thomson, R. E., &  
 529 Lorenzo, E. D. (2008). Modeling the generation of the Juan de Fuca Eddy. *J.  
 530 Geophys. Res.*, *113*(C3). doi: 10.1029/2006jc004082
- 531 Freeland, H., & Denman, K. (1982). A topographically controlled upwelling ceter off  
 532 southern Vancouver Island. *J. Mar. Res.*, *40*(4), 1069–1093.
- 533 Freeland, H., & McIntosh, P. (1989). The vorticity balance on the southern British Columbia  
 534 continental shelf. *Atmosphere–Ocean*, *27*(4), 643–657.
- 535 Harris, C. R., Millman, K. J., van der Walt, S. J., Gommers, R., Virtanen, P., Cournapeau,  
 536 D., ... Oliphant, T. E. (2020, sep). Array programming with NumPy. *Nature*,  
 537 *585*(7825), 357–362. Retrieved from <https://doi.org/10.1038%2Fs41586-020-2649-2>  
 538 doi: 10.1038/s41586-020-2649-2
- 539 Hickey, B., Thomson, R., Yih, H., & LeBlond, P. (1991). Velocity and temperature fluctu-  
 540 ations in a buoyancy-driven current off Vancouver Island. *J. Geophys. Res.*, *96*(C6),  
 541 10,507–10,538.
- 542 Hoyer, S., & Hamman, J. (2017, apr). xarray: N-d labeled arrays and datasets in python.  
 543 *Journal of Open Research Software*, *5*(1), 10. Retrieved from <https://doi.org/10.5334%2Fjors.148>  
 544 doi: 10.5334/jors.148
- 545 Hu, C., Lee, Z., & Franz, B. (2012). Chlorophyll a algorithms for oligotrophic oceans: A  
 546 novel approach based on three-band reflectance difference. *J. Geophys. Res.*, *117*(C1).  
 547 doi: 10.1029/2011jc007395
- 548 Ikeda, M., & Emery, W. J. (1984). A continental shelf upwelling event off Vancouver  
 549 Island as revealed by satellite infrared imagery. *J. Mar. Res.*, *42*(2), 303–317. doi:  
 550 10.1357/002224084788502774
- 551 Ikeda, M., Mysak, L. A., & Emery, W. J. (1984). Observation and modeling of satellite-  
 552 sensed meanders and eddies off Vancouver Island. *J. Phys. Oceanogr.*, *14*(1), 3–21.  
 553 doi: 10.1175/1520-0485(1984)014<0003:omoss>2.0.co;2
- 554 Klymak, J. M., Crawford, W., Alford, M. H., MacKinnon, J. A., & Pinkel, R. (2015).  
 555 Along-isopycnal variability of spice in the North Pacific. *J. Geophys. Res.*, *2169*-9291.  
 556 doi: 10.1002/2013JC009421
- 557 Klymak, J. M., Shearman, R. K., Gula, J., Lee, C. M., D'Asaro, E. A., Thomas, L. N., ...  
 558 others (2016). Submesoscale streamers exchange water on the north wall of the Gulf  
 559 Stream. *Geophys. Res. Lett.*. doi: 10.1002/2015GL067152
- 560 MacFadyen, A., & Hickey, B. M. (2010). Generation and evolution of a topographically  
 561 linked, mesoscale eddy under steady and variable wind-forcing. *Cont. Shelf Res.*,  
 562 *30*(13), 1387–1402. doi: 10.1016/j.csr.2010.04.001
- 563 Mackas, D. L., Denman, K. L., & Bennett, A. F. (1987). Least squares multiple tracer  
 564 analysis of water mass composition. *J. Geophys. Res.*, *92*(C3), 2907–2918.
- 565 Mackas, D. L., & Yelland, D. R. (1999, nov). Horizontal flux of nutrients and plankton  
 566 across and along the British Columbia continental margin. *Deep Sea Res. II*, *46*(11-  
 567 12), 2941–2967. doi: 10.1016/s0967-0645(99)00089-2
- 568 NASA Ocean Biology Processing Group. (2017). *MODIS-aqua level 3 mapped chloro-  
 569 phyll data version r2018.0*. NASA Ocean Biology DAAC. Retrieved from <https://oceancolor.gsfc.nasa.gov/data/10.5067/AQUA/MODIS/L3M/CHL/2018>  
 570 doi: 10.5067/AQUA/MODIS/L3M/CHL/2018
- 571 NASA Ocean Biology Processing Group. (2019). *MODIS-aqua level 3 mapped SST data  
 572 version r2019.0*. NASA Ocean Biology DAAC. Retrieved from [https://oceandata.sci.gsfc.nasa.gov/ob/getfile/AQUA\\_MODIS](https://oceandata.sci.gsfc.nasa.gov/ob/getfile/AQUA_MODIS)
- 573 OSI SAF. (2015). *GHRSST level 2p sub-skin sea surface temperature from the Advanced  
 574 Very High Resolution Radiometer (AVHRR) on Metop satellites (currently Metop-A)  
 575 (GDS V2) produced by OSI SAF*. NASA Physical Oceanography DAAC. Retrieved  
 576 from [https://podaac.jpl.nasa.gov/dataset/AVHRR\\_SST\\_METOP\\_A-OSISAF-L2P-v1.0](https://podaac.jpl.nasa.gov/dataset/AVHRR_SST_METOP_A-OSISAF-L2P-v1.0)  
 577 doi: 10.5067/GHAMA-2PO02
- 578 Pelland, N. A., Eriksen, C. C., & Lee, C. M. (2013). Subthermocline eddies over the  
 579 washington continental slope as observed by seagliders, 2003-09. *J. Phys. Oceanogr.*  
 580 doi: 10.1175/JPO-D-12-086.1

- 583 Relvas, P., & Barton, E. D. (2005). A separated jet and coastal counterflow during upwelling  
584 relaxation off Cape São Vicente (Iberian Peninsula). *Cont. Shelf Res.*, *25*(1), 29–49.  
585 doi: 10.1016/j.csr.2004.09.006
- 586 Sahu, S., Allen, S. E., Saldías, G. S., Klymak, J. M., & Zhai, L. (2022, mar). Spatial and  
587 temporal origins of the La Perouse low oxygen pool: A combined lagrangian statistical  
588 approach. *J. Geophys. Res.*, *127*(3). doi: 10.1029/2021jc018135
- 589 Thomson, R. E., & Gower, J. F. R. (1998, feb). A basin-scale oceanic instability event in  
590 the gulf of alaska. *J. Geophys. Res.*, *103*(C2), 3033–3040. doi: 10.1029/97jc03220
- 591 Thomson, R. E., Hickey, B. M., & LeBlond, P. H. (1989). The Vancouver Island Coastal  
592 Current: Fisheries barrier and conduit. In R. J. Beamish & G. A. McFarlane (Eds.),  
593 *Effects of ocean variability on recruitment and an evaluation of parameters used in  
594 stock assessment models*. Fisheries and Oceans Canada.
- 595 Thomson, R. E., & Krassovski, M. V. (2015, dec). Remote alongshore winds drive variability  
596 of the California Undercurrent off the British Columbia–Washington coast. *J. Geophys.  
597 Res.*, *120*(12), 8151–8176. doi: 10.1002/2015jc011306
- 598 Weaver, A. J., & Hsieh, W. W. (1987). The influence of buoyancy flux from estuaries  
599 on continental shelf circulation. *J. Phys. Oceanogr.*, *17*, 2127–2140. doi: 10.1175/  
600 1520-0485(1987)017<2127:TIOBFF>2.0.CO;2